J. Membrane Biol. 199, 85–98 (2004)
DOI: 10.1007/s00232-004-0679-6

The Journal of
Membrane
Biology

© Springer-Verlag New York, LLC 2004

Control of Epithelial Ion Transport by Cl^- and PDZ Proteins

R. Schreiber[1], A. Boucherot[1], B. Mürle[1], J. Sun[2], K. Kunzelmann[1]
[1]Institut für Physiologie, Universität Regensburg, Universitätsstraße 31, D-93053 Regensburg, Germany
[2]Department of Physiology and Pharmacology, University of Queensland, QLD, Australia

Received: 28 November 2003/Revised: 29 March 2004;

Abstract. Inhibition of epithelial Na^+ channels (ENaC) by the cystic fibrosis transmembrane conductance regulator (CFTR) has been demonstrated previously. Recent studies suggested a role of cytosolic Cl^- for the interaction of CFTR with ENaC, when studied in *Xenopus* oocytes. In the present study we demonstrate that the Na^+/H^+-exchanger regulator factor (NHERF) controls expression of CFTR in mouse collecting duct cells. Inhibition of NHERF largely attenuates CFTR expression, which is paralleled by enhanced Ca^{2+}-dependent Cl^- secretion and augmented Na^+ absorption by the ENaC. It is further demonstrated that epithelial Na^+ absorption and ENaC are inhibited by cytosolic Cl^- and that stimulation by secretagogues enhances the intracellular Cl^- concentration. Thus, the data provide a clue to the question, how epithelial cells can operate as both absorptive and secretory units: Increase in intracellular Cl^- during activation of secretion will inhibit ENaC and switch epithelial transport from salt absorption to Cl^- secretion.

Key words: CFTR — ENaC — Intracellular chloride — PDZ domain — NHERF — Epithelial transport

Introduction

The cystic fibrosis transmembrane conductance regulator (CFTR) is a cAMP-regulated Cl^- channel and a regulator of other channels [26]. Well examined and pathophysiologically most relevant is the inhibition of amiloride-sensitive epithelial Na^+ channels (ENaC) by CFTR [26]. Due to the CFTR defect and the lack of inhibition of ENaC, amiloride-sensitive Na^+ transport is enhanced in both, airways and colon of CF patients [1, 29, 30]. It has been shown previously that CFTR contains a common site for protein interaction at the very C-terminal end of the protein, a so-called PSD-95/DLG/ZO-1 (PDZ)-binding domain. Binding of regulatory PDZ domain proteins to this C-terminal end of CFTR, like the Na^+/H^+-exchanger regulator factor (NHERF), the hydrophilic PDZ protein CAP70 or CAL, has been demonstrated [5, 46, 47]. The PDZ domain is essential for proper expression of CFTR in the apical plasma membrane of respiratory epithelial cells [32, 33]. Thus, CFTR is anchored to the apical membrane via cytoskeletal interaction with the ezrin-binding phosphoprotein EBP50 [41]. Moreover, ezrin may function as an A kinase anchoring protein (AKAP), thereby linking protein kinase to CFTR and thus facilitate protein kinase A-dependent activation of CFTR [42]. The NHERF1 homologue E3KARP (NHERF2, TKA-1, SIP-1) mediates the association of ezrin and PKA with CFTR in airway cells [43]. Both NHERF1 and NHERF2 have been shown recently to bind to β_2 adrenergic and P2Y receptors and to interact with CIC-3B Cl^- channels [12, 35, 45]. Moreover, Na^+/HCO_3^- cotransport via NBC3 is linked via the PDZ-binding motif [36]. Thus, NHERF serves as a multifunctional adapter protein, essential for intracellular signaling. However, when expressed in non-polar *Xenopus* oocytes, the PDZ domain is neither required for CFTR expression nor for inhibition of ENaC [2]. As shown in these studies, an increase in the intracellular Cl^- concentration $[Cl^-]_i$ during activation of CFTR or via other Cl^- channels coexpressed with ENaC may cause inhibition of ENaC in *Xenopus* oocytes [2, 3, 19, 22].

Albeit substantial work has been done in *Xenopus* oocytes and other non-polarized cells, very little is known about the role of PDZ-binding domains and

Abbreviations: cAMP, cyclic adenosine monophosphate; CFTR, cystic fibrosis transmembrane conductance regulator; ENaC, epithelial Na^+ channel; IBMX 3-isobutyl-1-methylxanthine; NHERF1, Na^+/H^+-exchanger regulator factor; TKA-1, tyrosine kinase activating protein.

Correspondence to: K. Kunzelmann; email: uqkkunze@mailbox.uq.edu.au

$[Cl^-]_i$ for regulation of ENaC and salt transport in polarized epithelial cells. We therefore examined the role of both NHERF1 and Cl^- in polarized grown mouse collecting duct cells. Using electrophysiological and optical methods we demonstrate that an increase in $[Cl^-]_i$ is controlling the quantity and direction of epithelial salt transport.

Materials and Methods

M1 Cell Culture and Antisense DNA

M-1 mouse cortical collecting duct cells were kindly provided by C. Korbmacher (Physiologisches Institut, Universität Erlangen, Germany) and were grown to confluence for 3–5 days on permeable supports (Millipore MA, Germany) coated with rat-tail collagen (Roche, Germany) or on glass cover slips in DMEM/F12 medium containing 10% PCS; glutamine, 2 mmol/liter; penicillin, 100,000 units/liter; streptomycin, 100,000 units/liter; and dexamethasone, 0.1 μmol/liter. The resistances of the monolayers grown on permeable supports were checked every day using a volt-Ω-meter (Millicell-ERS, Millipore, Germany). Usually, monolayers with transepithelial resistances of around 1.5–2 kΩ were used for the experiments. Calu-3 cells were kindly provided by Dr. M. Hug (University Freiburg, Germany) and were kept in DMEM/F12 medium containing 15% FCS, glutamine, 2 mmol/liter; penicillin, 100,000 units/liter; streptomycin, 100,000 units/liter. For suppression of NHERF-1 expression, M1 cells grown on permeable supports were incubated for three days in a medium containing either stabilized antisense (5′-gtccgcgctcatcttgtt-3′) or missense (5′-gcaggcgcgagtagaacaag-3′) oligonucleotides (10 μmol/l) for mouse NHERF-1.

Western Blots and Immunocytochemistry of NHERF-1 and CFTR

Cells were lysed in sample buffer containing 10% SDS and 100 mmol/l DTT. Protein concentrations were determined according to a modified Laury method. Lysates containing 20 μg protein were subjected to SDS-polyacrylamide gel electrophoresis (SDS-PAGE) and analyzed by Western blotting as described previously [4]. Proteins were separated by 7% (CFTR) SDS-PAGE, transferred to nitrocellulose membranes (Bio-Rad, Hercules, CA) and bound antibodies were detected by enhanced chemiluminescence (Amersham, ArLington Heights, IL). A mouse monoclonal antibody (anti-CFTR [CF3], abcam, UK) was used for detection of CFTR by Western blotting. For immunocytochemistry, the M3A7 anti-CFTR antibody was kindly provided by Prof. J. Riordan, MAYO Clinic Scottsdale, Scottsdale, AZ) [15]. The rabbit anti NHERF-1 antibody was kindly provided by E.J. Weinman (John Hopkins University, Baltimore, USA). Horseradish peroxidase (HRPO)-conjugated and FITC-conjugated goat anti-mouse antibodies were obtained from Southern Biotechnology Associates (Birmingham, AL). The Cy3-labeled goat anti-rabbit antibody was obtained from Zymed Laboratories (South San Francisco, CA). M1 cells grown on glass cover slips were washed three times in PBS and fixed in methanol at −20°C. After washing in PBS, cells were incubated for 10 min in blocking buffer containing 10% BSA and 10% fish skin gelatin (both from Sigma, Australia). Cells were incubated overnight at 4°C in blocking solution, containing primary antibodies in 1:100 dilution. Subsequently, cells were washed again in PBS, then incubated with FITC- or Cy3-linked secondary antibodies for 45 min at 37°C. Tissues were counterstained with 4′,6-diamidino-2-phenylindole dihydrochloride (DAPI) solution (Sigma, Australia) and embedded in Mowiol (Sigma, Australia). Immunofluorescence was observed using an Olympus AX70 (Olympus Optical, Australia) microscope equipped with Uplan Apo 100×/1.35 and Uplan Apo 60×/1.40/0.17 objectives. Excitation wavelength for FITC and Cy-3 were 490 and 550 nm, respectively. FITC and Cy-3 fluorescence were observed at emission wavelengths of 515–550 and ≥580 nm.

RT-PCR Analysis

Total RNA was isolated from mouse total kidney and M1 cells grown for 5 and 14 days, respectively, using NucleoSpin RNAII (Macherey and Nagel, Düren, Germany). Total RNA was reverse-transcribed at 37°C for 1 h by using random primer and reverse transcriptase Superscript II (Life Technologies). Sequences specific for NKCC1 were amplified by PCR (94°C for 2 min; 35 cycles: 94°C for 30 s, 52°C for 1 min and 72°C for 1 min; 72°C for 10 min) using sense (s) 5′-GCGAGAAGGTGCACAATAC-3′ and antisense (as) 5′-CTGTACGGCTCGATCATGTC-3′ primers and Taq DNA Polymerase from Promega.

Ussing-Chamber Recordings

M1 cells were grown to confluence on permeable supports as described above. Inserts were mounted into a perfused Ussing chamber. The apical and basolateral surfaces of the epithelium were perfused continuously at a rate of 10 ml/min (chamber volume 2 ml). The bath solution contained (mmol/liter): NaCl, 145; KH_2PO_4, 0.4; K_2HPO_4, 1.6; D-glucose, 5; $MgCI_2$, 1; HEPES 5; and Ca-gluconate, 1.3, pH 7.4. Bath solutions were maintained at 37°C. Experiments were carried out under open-circuit conditions. Values for transepithelial potential differences (V_{te}) were referred to the serosal side of the epithelium. Currents were regarded as positive when conventional current flowed from the apical to the serosal side of the epithelium. The transepithelial resistance (R_{te}) was determined by applying short (1 s) current pulses ($I = 0.5$ μA), and the equivalent short-circuit current (I_{sc}) was calculated from V_{te} and R_{te} using Ohm's law.

Patch-Clamp Experiments

Cell culture dishes were mounted on the stage of an inverted microscope (IM35, Zeiss, Oberkochen, Germany) and kept at 37°C. The bath was continuously perfused with Ringer solution at a rate of about 10 ml/min. Patch-clamp experiments were performed in the fast whole-cell configuration according to [20]. The patch pipettes had an input resistance of 2–4 MΩ when filled with a solution containing (mmol/l) KCl 30, K-gluconate 95, NaH_2PO_4 1.2, Na_2HPO_4 4.8, EGTA 1, $CaCl_2$ 0.726, $MgCl_2$ 1.034, D-glucose 5, ATP 1 (32 Cl). The Cl^- concentration was adjusted to 2, 32 and 127 mmol/l by replacing appropriate amounts of Cl^- by gluconate. The pH was adjusted to 7.2, the Ca^{2+} activity was 0.1 μmol/l. The access conductance was measured continuously and was between 30 and 120 nS. Currents (voltage clamp) and voltages (current clamp) were recorded using a patch-clamp amplifier (EPC 7, List Medical Electronic, Darmstadt, Germany) and data were stored continuously on a computer hard disc. In regular intervals, membrane voltages (V_c) were clamped in steps of 10 mV from −100 mV to +40 mV. Membrane conductance G_m was calculated from the measured I and V_c values according to Ohm's law [20]. CFTR Cl^- currents were activated by 3-isobutyl-1-methylxanthine (IBMX; 100 μM) and forskolin (2 μM) (Sigma, Deisenhofen, Germany).

YFP-Fluorescence and Detection of Intracellular Cl^- Concentrations

Mouse kidney cortical collecting duct (M1) cells were grown on glass coverslips and transfected with pcDNA3.1(+) EYFP-V163S

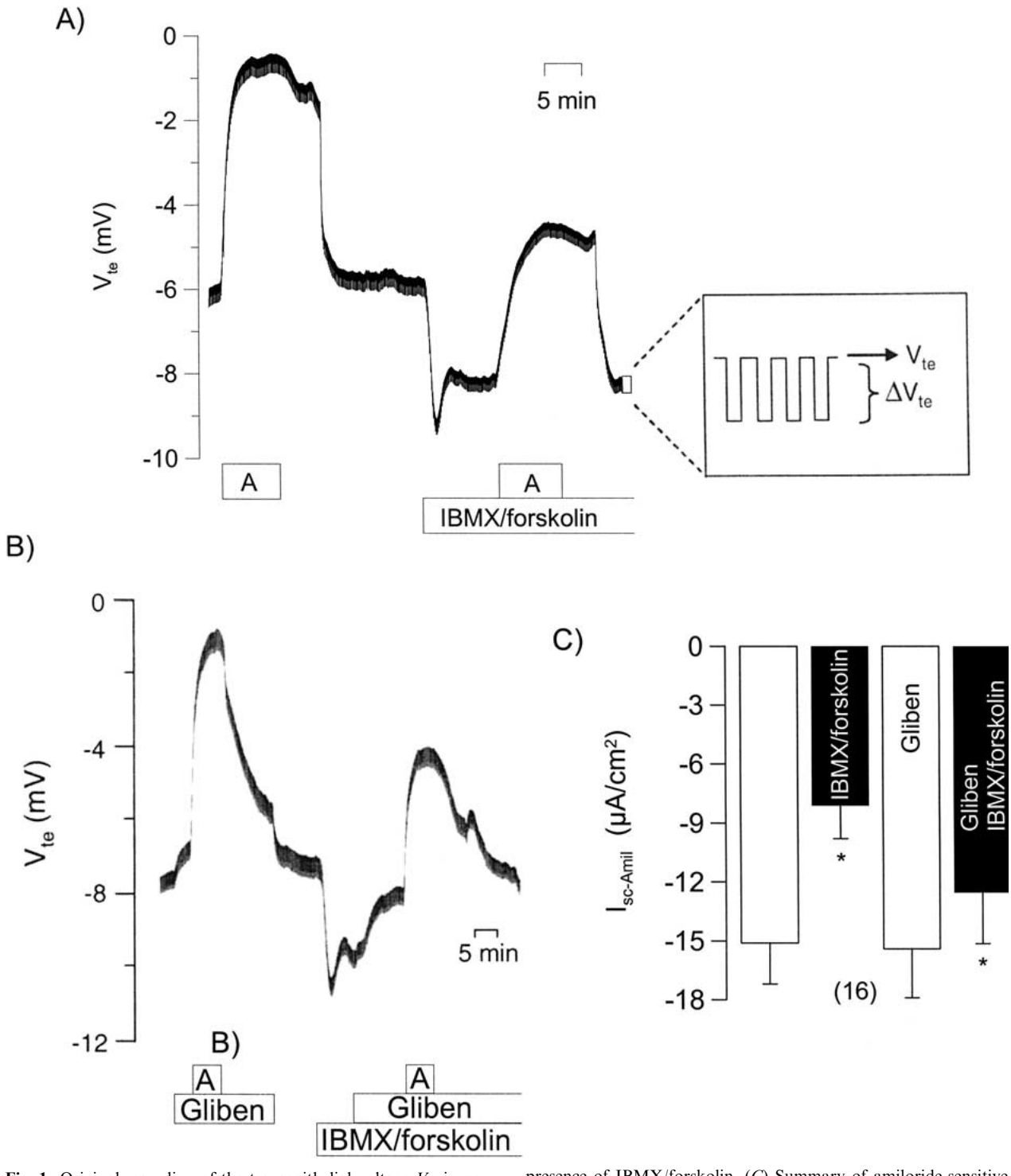

Fig. 1. Original recording of the transepithelial voltage V_{te} in polarized M1 cells. (*A*) Continuous recording of V_{te} and voltage deflection (ΔV_{te}) induced by pulsed current injection. Effects of amiloride (*A*, 10 µmol/l) and stimulation with IBMX/forskolin (100 µmol/l/2 µmol/l) on V_{te}. (*B*) Continuous recording of the effects of amiloride and glibenclamide (*Gliben*, 100 µmol/l) in the absence or presence of IBMX/forskolin. (*C*) Summary of amiloride-sensitive equivalent short-circuit currents ($I_{sc\text{-}Amil}$) before and after stimulation with IBMX/forskolin and in the absence or presence of glibenclamide. Asterisk indicates significant difference compared to control (paired *t*-test). (16) = number of experiments.

[9] using lipofectamine (Invitrogen) according to the manufacturer's protocol. The EYFP-V163S plasmid was kindly provided by A. Verkman (USCF, USA). Two to three days after transfection, cells were mounted under an inverted microscope IM35 (Zeiss, Germany) and perfused with a ringer solution (mmol/l: NaCl 145; KH_2PO_4 0.4; K_2HPO_4 1.6; glucose 5; $MgCl_2$ 1; Ca^{2+}-gluconate 1.3). For single-cell measurements the excitation wavelength was 500 nm, using a polychromatic illumination system for microscopic

fluorescence measurement (T.I.L.L. Photonics, Germany) and light emission was measured at 535 ± 15 nm with a photomultiplier detector (SF, Zeiss). For in vivo calibration of the Cl^- sensitivity of EYFP-V163S, a high-potassium buffer was used (mmol/l: K^+ 100; Na^+-gluconate 38, variable Cl^- concentrations with remaining anion being gluconate, HEPES 20; Ca^{2+}-gluconate 0.5; $MgSO_4$ 0.5, pH 7.4) containing nigericin (5 μmol/l), valinomycin (5 μmol/l), carbonyl cyanide 3-chlorophenylhydrazone (CCCP, 5 μmol/l), tributylinchlorid (10 μmol/l) and forskolin (2 μmol/l). To estimate chloride fluxes, cells were perfused with Ringer solution containing 5 mmol/Cl^-. Initial changes of fluorescence intensity with time in the presence or absence of IBMX (0.1 mmol/l) and forskolin (2 μmol/l) were calculated through linear regression.

Materials and Statistical Analysis

All compounds used were of highest available grade of purity. 3-Isobutyl-1-methylxanthine (IBMX), forskolin, amiloride, nigericin, valinomycin, CCCP, glibenclamide, bumetanide, cyclopiazonic acid, 4,4′-diisothiocyanatostilbene-2,2′-disulfonic acid (DIDS) were all from Sigma (Deisenhofen, Germany). All other chemicals were obtained from Merck (Darmstadt, Germany). Paired or unpaired Student's *t*-tests were used for statistical analysis, P values < 0.05 were accepted to indicate statistical significance (*).

Results

Amiloride-sensitive I_{SC} are Inhibited by CFTR in M1 Cells

After mounting M1 monolayers in the perfused Ussing chamber, a transepithelial voltage (V_{te}) of −8.2 ± 0.62 mV was measured and an equivalent short-circuit current (I_{sc}) of −17.2 ± 0.93 μA/cm² (n = 16) was calculated from the voltage deflections (ΔV_{te}) induced by pulsed current injection (0.5 μA). Short-circuit currents were dominated by electrogenic Na^+ absorption, since 10 μmol/l amiloride reduced I_{sc} reversibly to −1.89 ± 0.19 μA/cm² (n = 16) (Fig. 1*A*). A biphasic response was observed when tissues were stimulated with IBMX (100 μmol/l) and forskolin (2 μmol/l): V_{te} and I_{sc} were transiently increased to −11.7 ± 0.94 mV and −22.1 ± 1.82 μA/cm² and returned to a steady-state V_{te} and I_{sc} of −9.9 ± 0.74 mV and −21.2 ± 1.92 μA/cm² (n = 16). Steady-state I_{sc} was due to activation of luminal CFTR Cl^- currents, since glibenclamide (100 μmol/l) reduced V_{te} (−8.9 ± 1.03 mV) and I_{sc} (−17.8 ± 1.32 μA/cm²) (n = 16). The effects of amiloride on V_{te} were reduced and thus amiloride-sensitive equivalent short-circuit currents ($I_{sc\text{-}Amil}$) were inhibited by IBMX/forskolin (Fig. 1*A,C*). This inhibitory effect on $I_{sc\text{-}Amil}$ was attenuated in the presence of glibenclamide, suggesting a role of CFTR for inhibition of ENaC by IBMX/forskolin (Fig. 1*B,C*).

Stimulation with IBMX and forskolin activated both transient and steady-state I_{sc}, which may be due to an increase in both intracellular Ca^{2+} and cAMP, respectively. This may activate Ca^{2+}-dependent Cl^- channels as well as CFTR. Such an increase in intracellular Ca^{2+} and stimulation of Cl^- secretion has been demonstrated for respiratory cells of cystic fibrosis patients and tracheas of CFTR knockout mice [11, 34, 38]. Along the same line, a mixed Ca^{2+}/cAMP response has been found for stimulation of basolateral adrenoceptors in M1 cells [7]. We examined the effects of IBMX/forskolin in the presence of cyclopiazonic acid (CPA, 10 μmol/l), which depletes

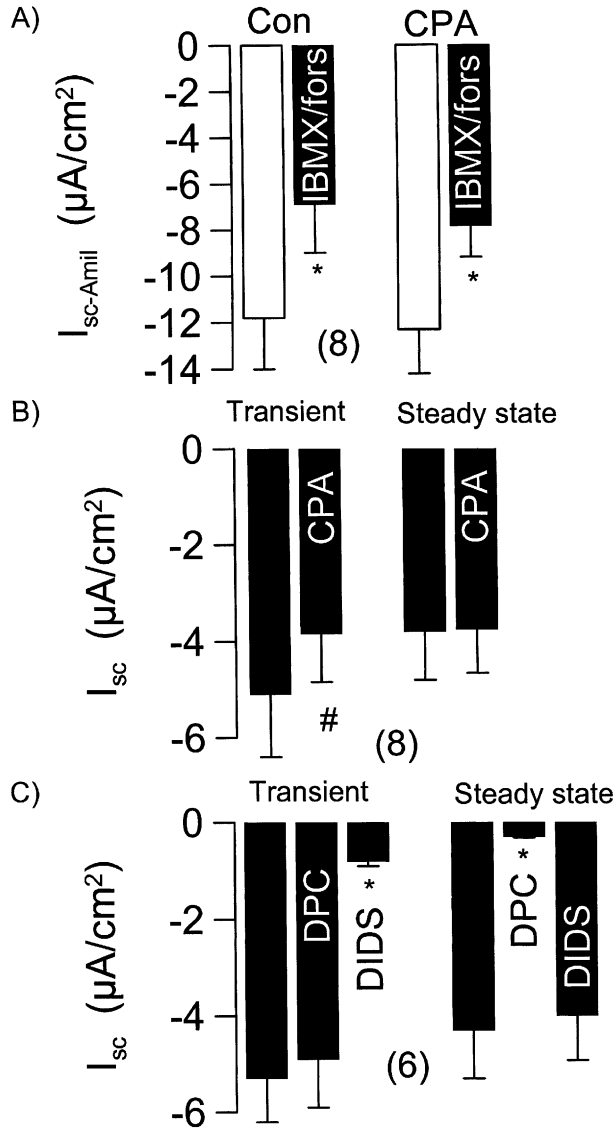

Fig. 2. (*A*) Summary of amiloride-sensitive equivalent short-circuit currents ($I_{sc\text{-}Amil}$) before and after stimulation with IBMX/forskolin and in the absence or presence of cyclopiazonic acid (CPA, 10 μmol/l). (*B*) Summary of the transient and steady-state equivalent short-circuit currents (I_{sc}) activated by IBMX/forskolin, and effects of CPA. (*C*) Summary of the transient and steady-state equivalent short-circuit currents (I_{sc}) activated by IBMX/forskolin and effects of diphenylamine-2-carboxylate (DPC, 1 mmol/l) and 4,4′-diisothiocyanatostilbene-2,2′-disulfonic acid (DIDS, 200 μmol/l). Asterisk indicates significant difference compared to control (without IBMX/forskolin, paired *t*-test). The number of experiments is given in parentheses.

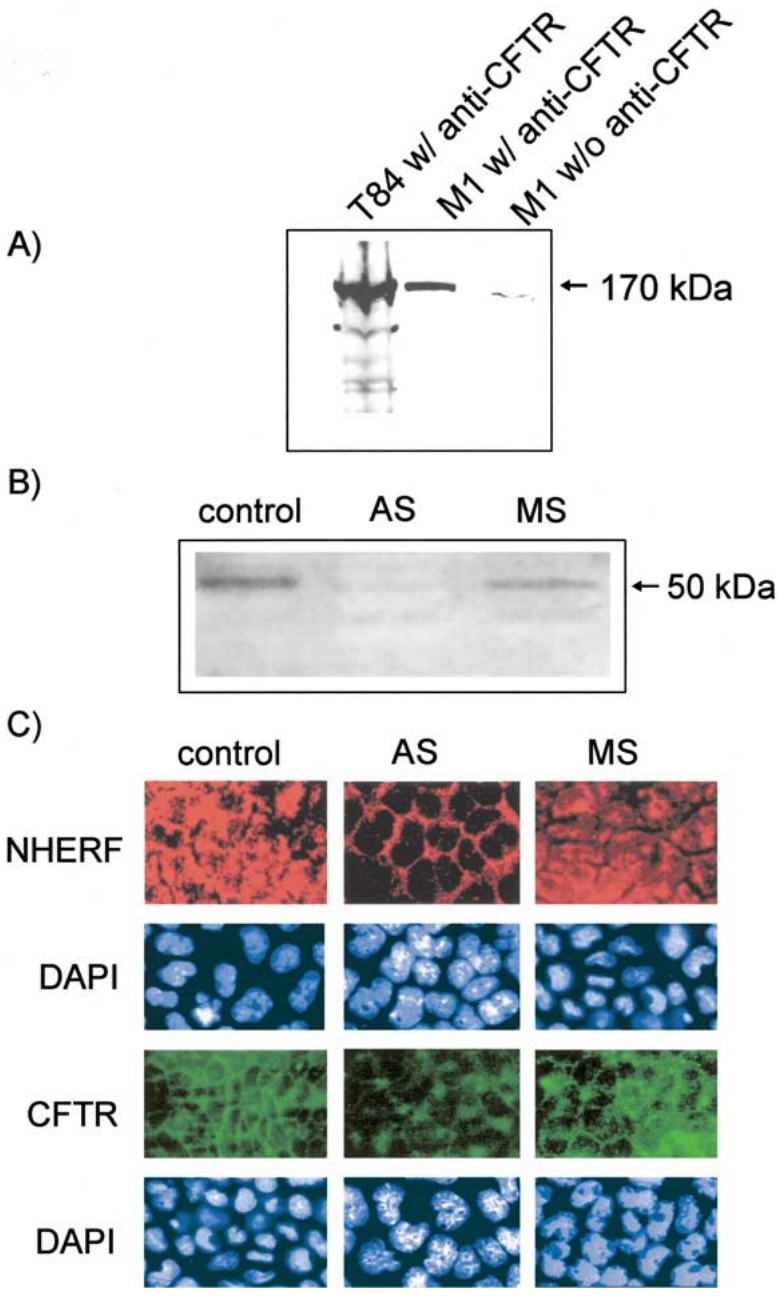

Fig. 3. Expression of the Na^+/H^+ exchanger regulatory factor 1 (NHERF) and CFTR and effects of treatment with NHERF-antisense (*AS*) and missense (*MS*) oligonucleotides. (*A*) Expression of CFTR in M1 cells as shown by Western blot analysis. For comparison, expression of CFTR in T_{84} colonic carcinoma cells is shown. Right lane shows a blot without (w/o) primary anti-CFTR antibody. (*B*) Expression of NHERF in M1 cells and effects of treatment with NHERF–antisense and missense oligonucleotides. (*C*) Immunocytochemistry of NHERF (*red*) and CFTR (*green*) in M1 control cells and M1 cells incubated with either NHERF–antisense or missense oligonucleotides. DAPI nuclei stain (*blue*) is shown below the individual cell preparations. Preparations treated without primary antibody (*control*) did not supply any fluorescence and were therefore omitted.

intracellular Ca^{2+} stores. Incubation with CPA did not affect baseline V_{te}, amiloride sensitive I_{sc}, or downregulation of $I_{sc\text{-}Amil}$ by IBMX/forskolin (Fig. 2*A*). However, the transient I_{sc} activated by IBMX/forskolin, was eliminated by CPA, while steady-state I_{sc} remained unaffected (Fig. 2*B*). Moreover, transient I_{sc} was also inhibited by 200 μmol/l 4,4′-diisothiocyanatostilbene-2,2′-disulfonic acid (DIDS), but was unaffected by 1 mmol/l DPC (or 100 μmol/l NPPB, *data not shown*). In contrast, steady-state I_{sc} was inhibited by DPC, but not by DIDS (Fig. 2*C*). Thus, stimulation with IBMX/forskolin does not only increase intracellular cAMP, but also leads to a transient increase in intracellular Ca^{2+} and Ca^{2+}-dependent Cl^- secretion.

In a separate set of experiments we examined whether delayed activation of luminal K^+ channels contributes to the transient voltage deflection induced by IBMX/forskolin. To that end we examined the effects of luminal application of K^+ channel inhibitors such as barium (5 mmol/l), charybdotoxin (100 nmol/l), apamin (100 nmol/l) and α-dendrotoxin (100 nmol/l). The inhibitors were examined in the absence or presence of IBMX/forskolin and before and after blocking Na^+ absorption by amiloride (10 μmol/l). Since we were unable to detect any effects of these

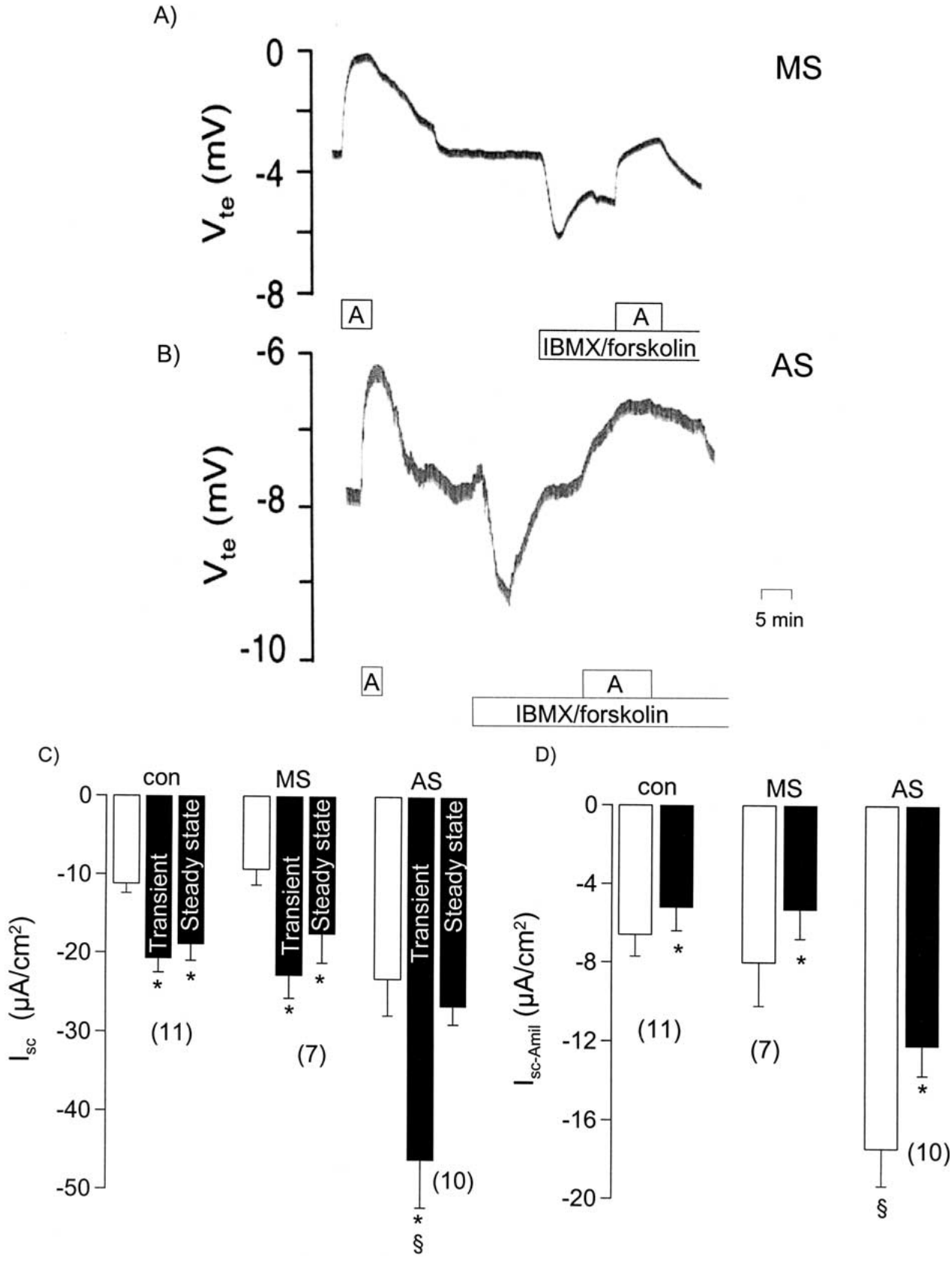
A)
MS
0
-4
-8
V_{te} (mV)
A
A
IBMX/forskolin
B)
AS
-6
-8
-10
V_{te} (mV)
5 min
A
A
IBMX/forskolin
C)
con
MS
AS
Transient
Steady state
I_{sc} (µA/cm²)
0
-10
-20
-30
-40
-50
(11)
(7)
(10)
*
§
D)
con
MS
AS
$I_{sc\text{-}Amil}$ (µA/cm²)
0
-4
-8
-12
-16
-20
(11)
(7)
(10)
*
§

Fig. 4. Original recording of the transepithelial voltage V_{te} in polarized M1 cells. Continuous recording of V_{te} and effects of amiloride (*A*, 10 μmol/l) and stimulation with IBMX/forskolin (100 μmol/1/2 μmol/1) on V_{te} in M1 cells treated with missense oligonucleotides (*A*) and NHERF-antisense oligonucleotides (*B*). (*C*) Summary of I_{sc} measured in control cells (*con*) and cells incubated with missense (*MS*) or antisense (*AS*) oligonucleotides, before (*white bars*) and after (*black bars*) stimulation with IBMX/forskolin. Transiently activated I_{sc} and steady-state I_{sc} activated by IBMX/forskolin are summarized separately. (*D*) Summary of $I_{sc\text{-}Amil}$ measured in control cells (*con*) and cells incubated in missense (*MS*) or antisense (*AS*) oligonucleotides, before (*white bars*) and after (*black bars*) stimulation with IBMX/forskolin. Asterisk indicates significant difference compared to control (without IBMX/forskolin, paired *t*-test) and § indicates significant difference compared to non-treated control cells (unpaired *t*-test). The number of experiments is given in parentheses.

inhibitors, we conclude that M1 cells do not possess a significant luminal K^+ conductance (*data not shown*). In contrast, basolateral application of 5 mmol/l Ba^{2+} inhibited both amiloride-sensitive and IBMX/forskolin-activated transport (*data not shown*).

Control of CFTR and ENaC by NHERF

CFTR has been shown to bind to and to be regulated by NHERF. To learn more about the potential role of NHERF for inhibition of amiloride-sensitive transport by CFTR in epithelial tissues, NHERF expression was suppressed by antisense oligonucleotides (AS). M1 cells do express CFTR, as detected by Western blotting (Fig. 3*A*). For comparison, expression of CFTR in T_{84} colonic carcinoma cells is shown [40]. Incubation of M1 cells by NHERF - AS for three days abolished NHERF expression, as shown by Western blot analysis, while missense oligonucleotides (MS) showed very little effect (Fig. 3*B*). Using immunocytochemistry, we further examined expression and localization of NHERF and CFTR in control cells and M1 cells treated with either AS or MS. As shown in Fig. 3*C*, control cells showed NHERF staining throughout the cells, while CFTR was localized mainly to the cell membrane. In AS-treated cells, expression of both NHERF and CFTR was reduced, while no obvious effects were found in cells treated with MS. For comparison, nuclei-staining with DAPI is included. Thus, NHERF is essential for expression and proper cellular localization of CFTR. These data confirm previous results, showing regulation of membrane expression of CFTR by binding to NHERF [14, 17].

We further asked whether the inhibition of amiloride-sensitive Na^+ currents by CFTR is different in cells treated with NHERF antisense. To that end, inhibition of amiloride-sensitive Na^+ transport by IBMX and forskolin was examined in control cells and cells that have been exposed to either AS or MS. As demonstrated in Fig. 4, both MS and AS-treated cells are dominated by amiloride-sensitive Na^+ absorption, which, however, is augmented in AS-treated cells. AS-treated cells show an augmented but only transient activation of I_{sc} by IBMX/forskolin (Fig. 4*A,B,C*). In both, MS- and AS-treated cells, $I_{sc\text{-}Amit}$ is inhibited by IBMX/forskolin. Taken together, Cl^- secretion by CFTR is abolished in cells lacking NHERF expression, while Ca^{2+}-activated secretion is enhanced. Ca^{2+}-activated Cl^- channels may compensate for the lack of CFTR and will maintain Cl^- transport and inhibition of ENaC. Thus, fractional inhibition of $I_{sc\text{-}Amit}$ during stimulation of the cells is similar (around 30%) in control, AS- and MS- treated cells.

Role of Cl^- for Inhibition of $I_{sc\text{-}AMIL}$

We previously found a role of Cl^- ions for inhibition of ENaC by CFTR [19, 39]. Thus, we examined how removal of extracellular (basolateral and luminal) Cl^- affects the downregulation of $I_{sc\text{-}Amil}$ by CFTR. To that end, we replaced 90 mmol/l of Cl^- in the extracellular bath solution by gluconate and activated CFTR Cl^- conductance. Under these conditions, no significant inhibition of $I_{sc\text{-}Amil}$ by CFTR was detected (Fig. 5*A*). Moreover, we exposed M1 cells to a hypertonic extracellular bath solution, by adding 80 mmol/l mannitol. This reduced $I_{sc\text{-}Amil}$ significantly and a further inhibition was observed during stimulation with IBMX and forskolin. In contrast, change from an isotonic solution, in which 40 mmol/l NaCl had been replaced by 80 mmol/l mannitol, to a hypotonic solution (removal of 80 mmol/l mannitol) had no impact on $I_{sc\text{-}Amil}$. In the presence of hypertonic media, no inhibition of $I_{sc\text{-}Amil}$ by activation of CFTR was observed (Fig. 5*B*). These experiments suggest that cell shrinkage, which is likely to be accompanied by an increase in $[Cl^-]_i$, does inhibit ENaC. The opposite, namely cell swelling and thus lowering of $[Cl^-]_i$, may antagonize CFTR-mediated inhibition of ENaC. Very similar results have been seen when mouse airways were stimulated with ATP in the presence of either hypertonic or hypotonic bath solutions [39].

During activation of Cl^- secretion, several transport proteins are activated and contribute to changes in $[Cl^-]_i$. Thus, secretory epithelial cells take up Cl^- from the basolateral side of the epithelium by the $Na^+/2Cl^-/K^+$-cotransporter (NKCC1). Indeed, mRNA encoding NKCC1 was amplified by RT-PCR in the present study in M1 cells cultured for different periods of time (Fig. 6*D*). Moreover, in transepithelial measurements, Cl^- secretion was completely blocked by the NKCC1 inhibitor bumetanide (basolateral, 100 μmol/l) (Fig. 6*A,B*). These results are in contrast to a previous study, which did not find evidence for the presence of NKCC1 in M1 cells [7]. Glibenclamide, when applied in the presence of bumetanide, was without any further effects on Cl^-

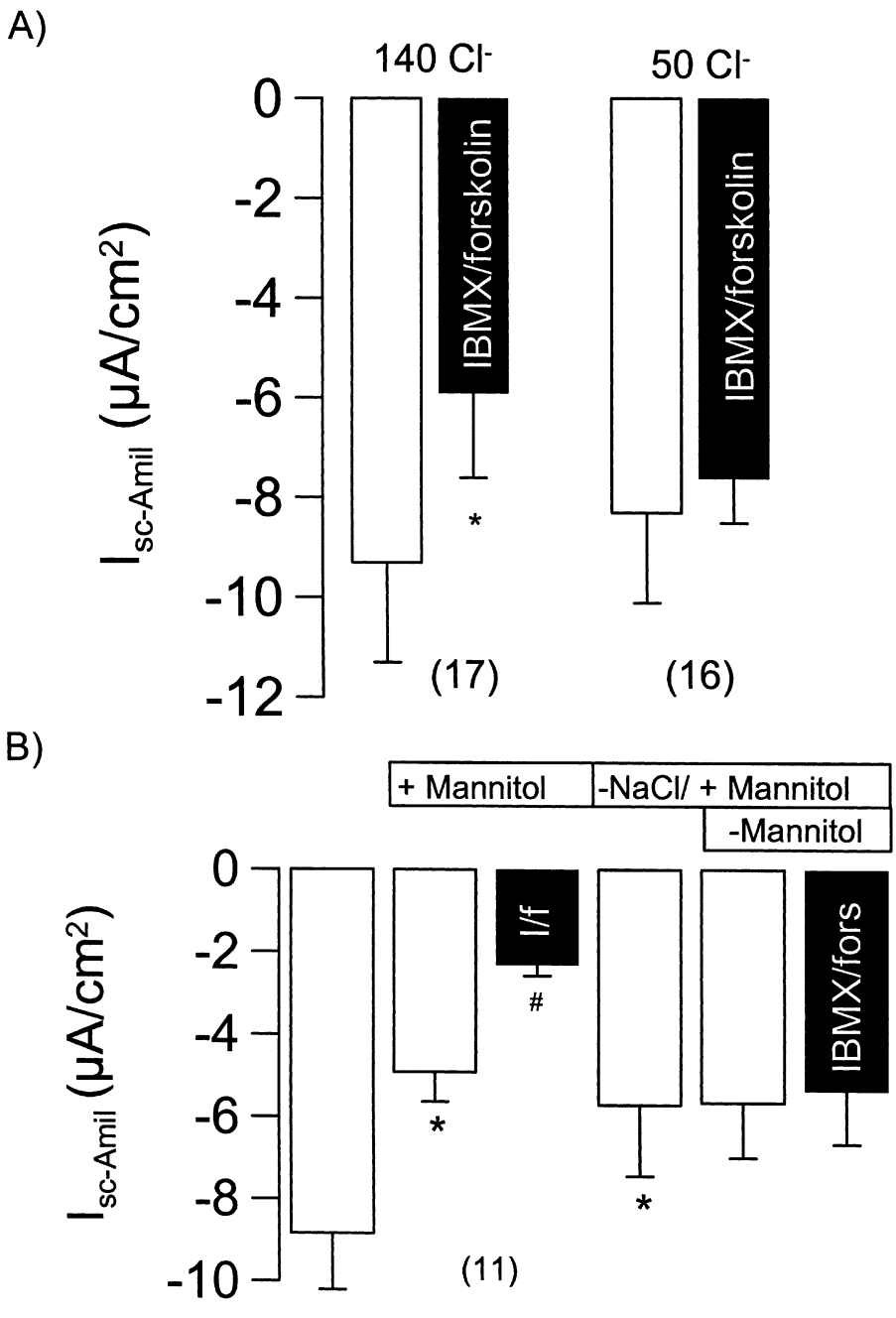

Fig. 5. Summary of $I_{sc\text{-}Amil}$ measured in M1 cells before (*white bars*) and after stimulation with IBMX/forskolin (*black bars*). (*A*) Cells were exposed either to Ringer solution containing 140 mmol/l Cl^- (140 Cl^-) or a buffer solution in which 90 mmol/l Cl^- has been replaced isosmotically by gluconate (50 Cl^-). (*B*) Cells were exposed to a hypertonic bath solution containing additional 80 mmol/l mannitol (*+ Mannitol*) or to a solution in which 40 mmol/l NaCl has been replaced isotonically by 80 mmol/l mannitol (*-NaCl/ + Mannitol*) or to a hypotonic bath solution (*-Mannitol*). Asterisk indicates significant difference compared to control Ringer solution; # indicates significant difference compared to control (without IBMX/forskolin, paired *t*-test). The number of experiments is given in parentheses.

secretion, which indicates the requirement of basolateral NKCC1 for Cl^- secretion in M1 cells. Noticeably, bumetanide blocked downregulation of ENaC by CFTR. This result indicates that Cl^- uptake by basolateral NKCC1 is essential for inhibition of $I_{sc\text{-}Amil}$ during cAMP-dependent stimulation of secretion in M1 cells.

Role of Cl^- as Determined by YFP Fluorescence and Patch-Clamp Experiments

Recent reports demonstrate the use of the yellow fluorescent protein YFP for detection of $[Cl^-]_i$ [9, 10, 13]. In order to assess putative changes in $[Cl^-]_i$ during activation of transport, we expressed YFP in M1 cells. The mutant EYFP–V163S was used for assessment of changes in $[Cl^-]_i$ during activation of CFTR by IBMX (100 µmol/l) and forskolin (2 µmol/l). Initially, a calibration curve was obtained, which showed an almost linear dependence of the fluorescence intensity from $[Cl^-]_i$ (Fig. 7*A*). During stimulation of the cells with IBMX and forskolin, the fluorescence was quenched due to increase in $[Cl^-]_i$, which caused a $3.1 \pm 3.37\%$ ($n = 22$) decrease of fluorescence intensity. This change in YFP fluorescence is equivalent to a change in the intracellular Cl^-

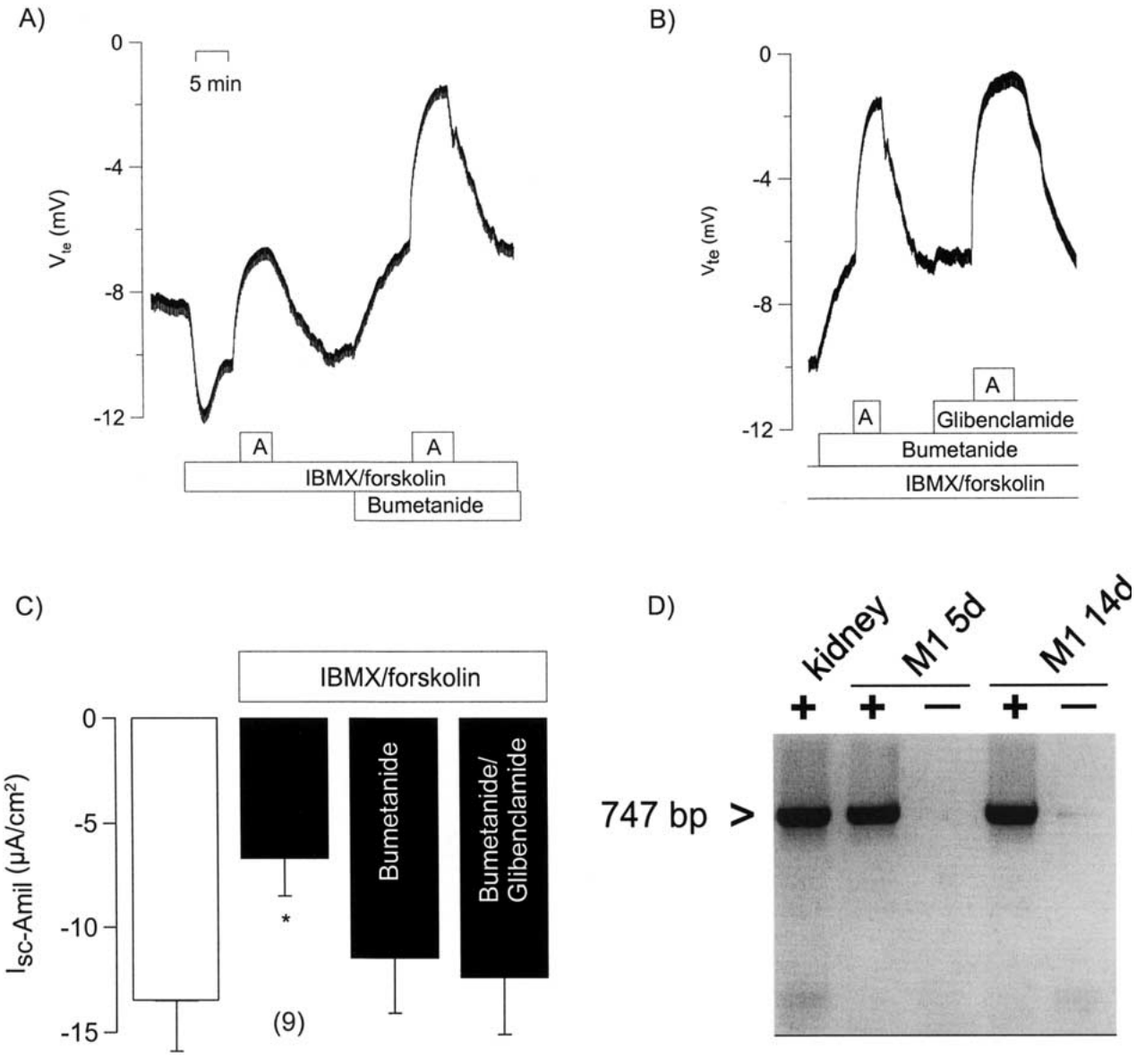

Fig. 6. (*A, B*) Original recording of the transepithelial voltage V_{te} in polarized M1 cells. Continuous recording of V_{te} and effects of amiloride (*A*, 10 μmol/l) and stimulation with IBMX/forskolin (100 μmol/l / 2 (μmol/l) in the absence or presence of bumetanide (100 μmol/l) (*A*) or bumetanide/glibenclamide (100 μmol/l) (*B*). (*C*) Summary of $I_{sc\text{-}Amil}$ measured before (*white bar*) and after stimulation with IBMX/forskolin in either absence or presence of bumetanide and bumetanide/glibenclamide. Asterisk indicates significant difference compared to control (without IBMX/forskolin, paired *t*-test). In parentheses, the number of experiments. (*D*) RT-PCR analysis of the expression of the $Na^+/2Cl^-/K^+$ cotransporter NKCC1 in kidney epithelial cells and M1 cells grown for either 5 or 14 days. An NKCC1-specific fragment (747 bp) was amplified in the presence (+) but not absence (−) of reverse transcriptase.

concentration of 16.8 ± 3.3 mmol/l. Replacing extracellular Ringer solution by a low (5 mmol/l) Cl^- solution induced an efflux of Cl^- and a dequenching of the fluorescence signal. The efflux was more pronounced, and thus the slope of the fluorescence increase was steeper, after stimulation of additional CFTR Cl^- channels with IBMX and forskolin (Fig. 7*B,C*). These data demonstrate that activation of CFTR Cl^- channels in absorptive M1 cells causes an increase in $[Cl^-]_i$ in the presence of physiological extracellular salt concentrations.

To provide further evidence for a Cl^--dependent regulation of ENaC, we performed fast whole-cell patch-clamp experiments, in which we used different pipette filling solutions, containing either 2, 32 or 127 mmol/l Cl^-. The extracellular bath solution was kept constant in these experiments and was a regular Ringer solution. In about 15% of all approaches, longer lasting stable tight seal recordings were obtained, which allowed for the entire experimental protocol.

The original whole-cell recording in Fig. 8*A* shows an inhibitory effect of amiloride, which is

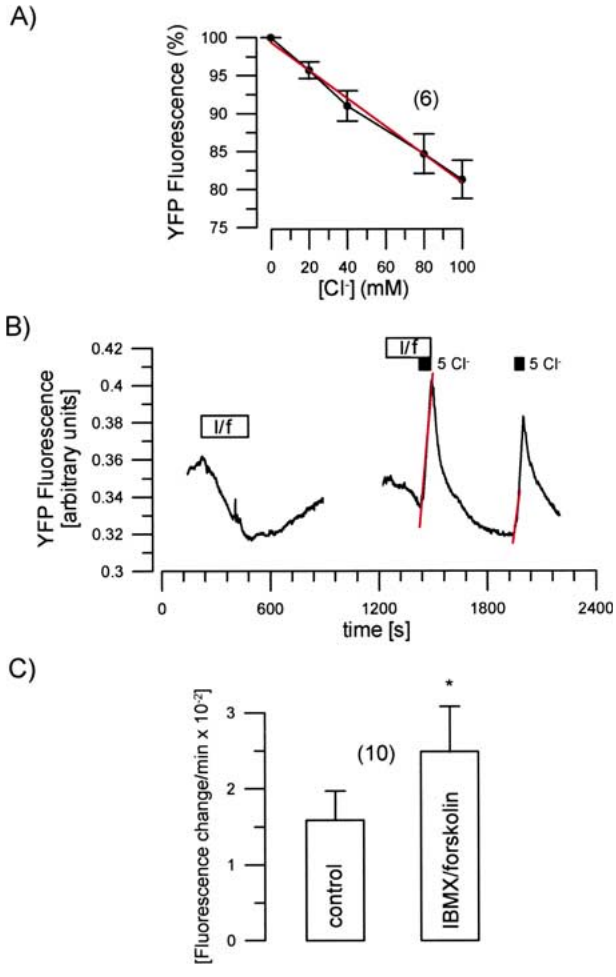

Fig. 7. (*A*) Calibration curve for Cl^- sensitivity of EYFP-V163S can be fit (*red line*) to an almost linear relationship of YFP fluorescence intensity and Cl^- concentration. (*B*) Original recording of the YFP fluorescence intensity. Quenching of the fluorescence by stimulation with IBMX and forskolin (*I*/*F*) in the presence of a high extracellular Cl^- concentration and dequenching of the fluorescence signal in the presence of a low (5 mmol/l) extracellular Cl^- concentration. (*C*) Summary of the change in fluorescence intensity during stimulation of M1 cells with IBMX and forskolin in the presence of a low Cl^- (5 mmol/l) bath solution. Asterisk indicates significant difference compared to control (without IBMX/forskolin, paired *t*-test). In parentheses, the number of experiments.

abolished after stimulation of the cell with IBMX and forskolin and activation of a Cl^- conductance. The insert indicates the voltage-clamp protocol used. Current voltage (*I*/*V*) relationships obtained in a typical experiment with a 32 mmol/liter Cl^- pipette filling solution, are shown in Fig. 8*B*. *I*/*V* curves were obtained under control conditions (*empty circles*), after applying 10 μmol/l amiloride (*filled circles*), after stimulation with IBMX/forskolin (*empty squares*) and after applying amiloride in the presence of IBMX/forskolin (*filled squares*). Fig. 8*C* summarizes amiloride-sensitive whole-cell currents (I_{Amil}), measured at a clamp voltage of −100 mV, and amiloride-induced hyperpolarization of the membrane voltage (ΔV_{Amil}). It is obvious that with increasing pipette Cl^- concentrations, both I_{Amil} and ΔV_{Amil} are reduced. This result suggests inhibition of ENaC by [Cl^-]. Remarkably, inhibition of I_{Amil} during stimulation of CFTR by IBMX and forskolin (*I*/*F*) (ΔI_{Amil}) was observed with either 2, 32 or 127 mmol/l Cl^- in the pipette filling solution (Fig. 8*D*). Taken together, ENaC currents are attenuated in the presence of a high $[Cl^-]_i$ and thus, accumulation of Cl^- during stimulation of epithelial cells coexpressing CFTR and ENaC may inhibit amiloride-sensitive Na^+ absorption.

Discussion

The Transport Properties of M1 Collecting Duct Cells and Inhibition of ENaC

Ion transport properties of M1 cells have been studied extensively. Apart from apical amiloride-sensitive Na^+ channels, which have been detected in patch-clamp experiments [27], K^+ currents [18] and Cl^- currents, activated by Ca^{2+} or cAMP [6, 7, 28, 31] have been found. We found Ca^{2+}- and cAMP- dependent Cl^- secretion in the present study and found further evidence for activation of Ca^{2+}-activated Cl^- channels by luminal ATP in unpublished experiments. Thus, M1 cells maintain both absorptive as well as secretory properties, similar to epithelial cells [24]. Because M1 cells express both ENaC and CFTR, interferences between both ion channels can be studied in polarized fashion. In fact, a recent patch-clamp study demonstrated activation of CFTR Cl^- currents in M1 cells, which is paralleled by inhibition of amiloride-sensitive Na^+ channels [28].

Fig. 8. Fast whole-cell patch-clamp experiments. (*A*) Original recording of the whole-cell current in an M1 cell, showing the effect of amiloride (10 (μmol/l), which was abolished after stimulation with IBMX (100 μmol/l) and forskolin (10 μmol/l). The membrane voltage was voltage-clamped from the zero-current membrane potential according to the protocol shown in the insert. (*B*) Current voltage (*I*/*V*) relationships obtained in a typical experiment using a pipette filling solution with 32 mmol/l Cl^-. *I*/*V* curves were obtained under control conditions (*empty circle*), after applying 10 μmol/l amiloride (*filled circles*), after stimulation with IBMX/forskolin (*empty squares*) and after applying amiloride in the presence of IBMX/forskolin (*filled squares*). (*C*) Summaries of amiloride-sensitive whole-cell currents (I_{Amil}) measured at a clamp voltage of −100 mV, and amiloride-induced hyperpolarization of the membrane voltage (ΔV_{Amil}) in fast whole-cell patch-clamp experiments. I_{Amil} and ΔV_{Amil} were determined in experiments using different pipette filling solutions with either 2, 32 or 127 mmol/l Cl^-. (*D*) Summary of the amount of I_{Amil} inhibited during stimulation of CFTR by IBMX and forskolin (*I*/*F*) (ΔI_{Amil}) in the presence of 2, 32 or 127 mmol/l Cl^- in the pipette solution. Asterisk indicates significant difference compared to control (without IBMX/forskolin, paired *t*-test). In parentheses, the number of experiments.

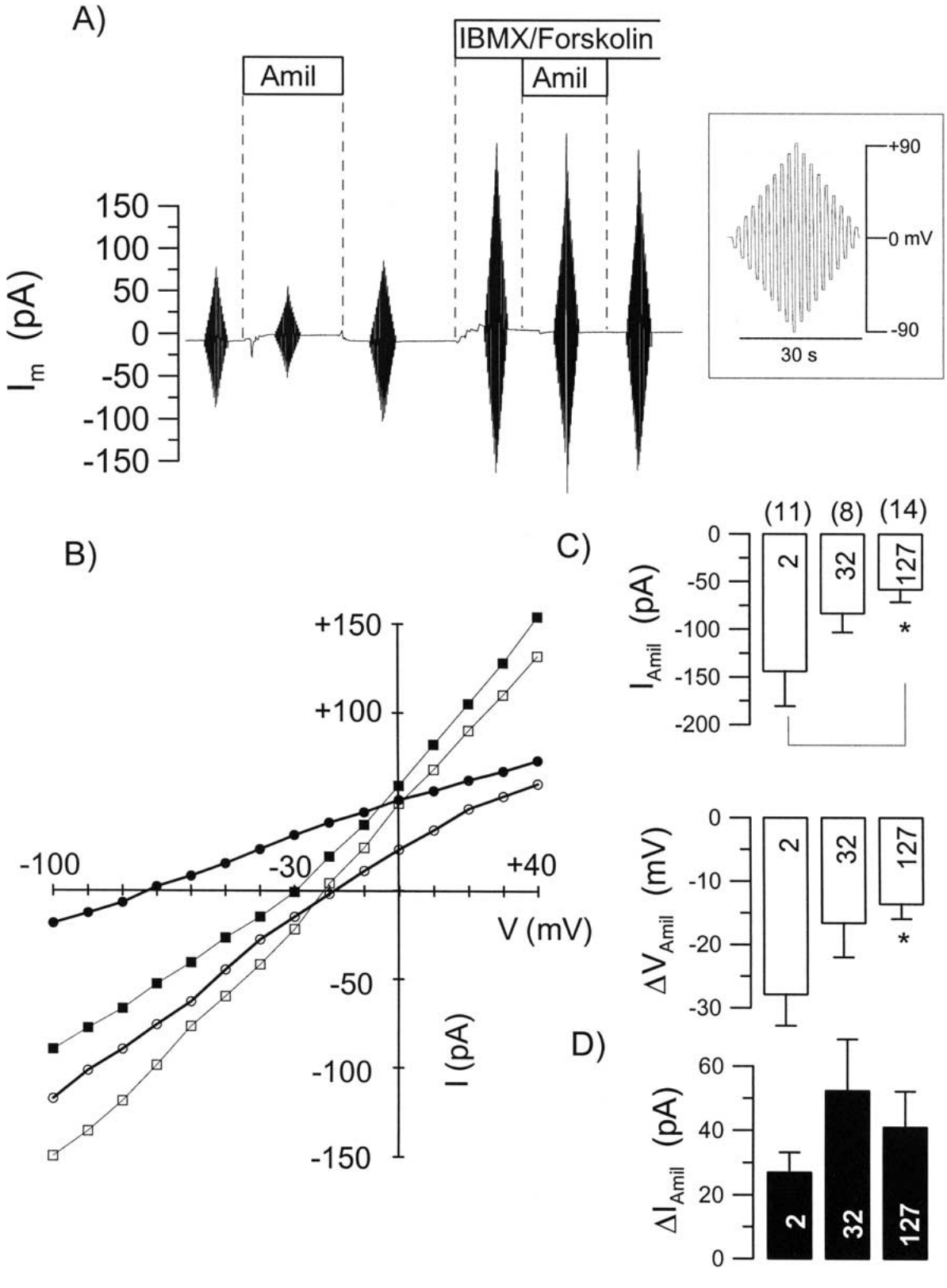
A)
Amil
IBMX/Forskolin
Amil
150
100
50
0
-50
-100
-150
I_m (pA)
+90
0 mV
-90
30 s
B)
+150
+100
-100
-30
+40
V (mV)
-50
-100
-150
I (pA)
C)
(11) (8) (14)
0
-50
-100
-150
-200
I_{Amil} (pA)
2
32
127
*
0
-10
-20
-30
ΔV_{Amil} (mV)
2
32
127
*
D)
60
40
20
0
ΔI_{Amil} (pA)
2
32
127

These results are confirmed in the present report. Interestingly, a basolateral $Na^+/K^+/2Cl^-$ cotransporter (NKCC1) was not detected in M1 cells previously [6, 7]. NKCC1, which is a hallmark of secretory epithelial cells, is thought to play a role for the uptake of Cl^- in the collecting duct [8, 16, 23]. The present RT-PCR analysis shows clear evidence for expression of NKCC1 in M1 cells, while functional expression is demonstrated by inhibition of secretion by blocking NKCC1 with bumetanide or azosemide.

Expression of transport proteins and thus the transport properties of M1 cells may largely depend on the culture conditions. This has been proposed previously [7, 18] and is further confirmed by the present study. Generally, we observed a decline in CFTR-mediated Cl^- secretion and an increase in transepithelial Na^+ absorption with age of the M1 cell culture, which is in line with previous results [7]. In the present study, we intended to examine the interaction between CFTR and ENaC in a polarized environment and therefore used M1 cells at an earlier stage (3–4 days), when they possess both, a large Na^+ transport by ENaC along with CFTR-dependent Cl^- secretion. We detected reversible inhibition of ENaC currents during activation of CFTR in M1 cells, similar to the results of a recent patch-clamp study on M1 cells grown on glass cover slips [28]. Inhibition of ENaC, however, was not observed on M1 cells grown on permeable supports for up to 12 days. This is probably due to the comparatively small Cl^- conductance activated by noradrenaline [7].

NHERF-1 May Control both CFTR and ENaC

The present data show blocking of NHERF-1 expression, which results in a decrease of CFTR expression as well as cAMP-dependent Cl^- secretion. These results are in line with the PDZ domain interaction, which controls the endocytic recycling pathway and the activity of CFTR [37, 44]. Moreover, two PDZ proteins, NHERF and CAL, have been shown to compete for binding at the PDZ binding domain of CFTR [5]. While binding to the Golgi-associated CAL protein inhibits membrane expression of CFTR and favors retention within the cell, binding to NHERF promotes cell surface expression and chloride currents [5]. As CAL shows a broad expression, including epithelial tissues from kidney, airways and colon, a similar scenario is likely to take place in M1 collecting duct cells.

Remarkably, we found an increase of amiloride-sensitive Na^+ transport in cells that have been treated with NHERF-antisense. This may indicate a lack of CFTR-dependent inhibition of ENaC. It may also reflect improved expression of ENaC in cells with reduced NHERF protein expression, or when Golgi retention proteins such as CAL preferentially bind to CFTR. Such a dynamic interaction between different PDZ domain proteins could also be the reason for the augmenting effects of ENaC-coexpression on CFTR Cl^- currents, as observed by some investigators [14, 17]. Moreover, suppression of CFTR expression by NHERF-antisense was paralleled by an augmented transient Ca^{2+}-activated Cl^- conductance. This result is reminiscent of the inhibition of endogenous Ca^{2+}-activated Cl^- conductance by CFTR in *Xenopus* ooctyes and bovine pulmonary artery endothelial cells [25, 48].

A main result of the present study is the reversible inhibition of ENaC currents by CFTR and its coupling to Cl^- transport. Previously, we reported Cl^--dependent inhibition of ENaC in *Xenopus* oocytes [2, 3, 19, 21, 39], while other data were obtained from mouse trachea [22]. The present patch-clamp data indicate inhibition of ENaC by a high Cl^- concentration in the patch-pipette filling solution. Further inhibition of I_{Amil} by stimulation with secretagogues in the presence of a high $[Cl^-]_i$ (pipette) may have different reasons, such as i) Cl^-independent effects of CFTR on ENaC, ii) inhomogeneous distribution of Cl^- with low $[Cl^-]_i$ in close proximity to the cell membrane, iii) electroneutral uptake of NaCl via parallel CFTR/ENaC shunts, or iv) Na^+ feedback inhibition of ENaC. The present data show an initial increase in $[Cl^-]_i$ upon stimulation of the cell by IBMX/forskolin. This initial increase may occur via luminal Cl^- channels as well as basolateral $Na^+/K^+/2Cl^-$ cotransporter. Cl^- may be taken up into the cell via CFTR during the onset of stimulation, since Cl^- is close to the electrochemical equilibrium and opening of CFTR will allow for electroneutral uptake of NaCl. Upon further increase of intracellular Cl^- and partial inhibition of ENaC, the electrochemical equilibrium for Cl^- will shift towards secretion.

According to the present results, NKCC1 is required for Cl^- secretion and is therefore likely to increase $[Cl^-]_i$. Since Ca^{2+}-dependent Cl^- transport is enhanced in NHERF1-AS treated cells, this may compensate for the lack of CFTR and will maintain Cl^- transport and inhibition of ENaC.

In summary, we propose a mechanism for the inhibition of ENaC by CFTR in polarized epithelial cells and how the epithelium may switch from salt absorption under baseline conditions to salt secretion after stimulation with secretagogues. An increase in intracellular Cl^- may play a crucial role, which is supported by the present patch-clamp recordings demonstrating inhibition of Na^+ currents by high $[Cl^-]_i$.

This work was supported by NHMRC 252823 and ARC A00104609, the Else Kröner-Fresenius Stiftung. The excellent technical assistance by Ms. Ernestine Tartler and Ms. Agnes Paech is gratefully acknowledged. We thank Prof. Alan Verkman and Dr. Ma for providing us with the YFP constructs and Prof E. Weinman for supplying the NHERF antibody.

References

1. Boucher, R.C., Cotton, C.U., Gatzy, J.T., Knowles, M.R., Yankaskas, J.R. 1988. Evidence for reduced Cl^- and increased Na^+ permeability in cystic fibrosis human primary cell cultures. *J. Physiol.* **405:**77–103
2. Boucherot, A., Schreiber, R., Kunzelmann, K. 2001. Role of CFTR's PDZ-binding domain, NBF1 and Cl^- conductance in inhibition of epithelial Na^+ channels in *Xenopus* oocytes. *Biochim. Biophys. Ada* **1515:**64–71
3. Briel, M., Greger, R., Kunzelmann, K. 1998. Cl^- transport by CFTR contributes to the inhibition of epithelial Na^+ channels in *Xenopus* ooyctes coexpressing CFTR and ENaC. *J. Physiol.* **508. 3:**825–836
4. Chang, X.-B., Tabcharani, J.A., Hou, Y.-X., Jensen, T.J., Kartner, N., Alon, N., Hanrahan, J.W., Riordan, J.R. 1993. Protein kinase A (PKA) still activates CFTR chloride channels after mutagenesis of all 10 PKA consensus phosphorylation sites. *J. Biol. Chem.* **268:**11304–11311
5. Cheng, J., Moyer, B.D., Milewski, M., Loffing, J., Ikeda, M., Mickle, J.E., Cutting, G.G., Li, M., Stanton, B.A., Guggino, W.B. 2002. A GOLGI associated PDZ domain protein modulates cystic fibrosis transmembrane regulator plasma membrane expression. *J. Biol. Chem.* **277:**3520–3529
6. Cuffe, J.E., Bielfeld-Ackermann, A., Thomas, J., Leipziger, J., Korbmacher, C. 2000. ATP stimulates Cl^- secretion and reduces amiloride-sensitive Na^+ absorption in M-1 mouse cortical collecting duct cells. *J. Physiol.* **524:**77–90
7. Cuffe, J.E., Howard, J.P., Bertog, M., Korbmacher, C. 2002. Basolateral adrenoceptor activation mediates noradrenaline-induced Cl^- secretion in M-1 mouse cortical collecting duct cells. *Pfluegers Arch.* **445:**381–389
8. Delpire, E., Rauchman, M.I., Beier, D.R., Hebert, S.C., Gullans, S.R. 1994. Molecular cloning and chromosome localization of a putative basolateral Na^+-K^+−$2Cl^-$ cotransporter from mouse inner medullary collecting duct (mlMCD-3) cells. *J. Biol. Chem.* **269:**25677–25683
9. Galietta, L.J., Haggie, P.M., Verkman, A.S. 2001. Green fluorescent protein-based halide indicators with improved chloride and iodide affinities. *FEBS Lett.* **499:**220–224
10. Galietta, L.J., Springsteel, M.F., Eda, M., Niedzinski, E.J., By, K., Haddadin, M.J., Kurth, M., Nantz, H., Verkman, A.S. 2001. Novel CFTR chloride channel activators identified by screening of combinatorial libraries based on flavone and benzoquinolizinium lead compounds. *J. Biol. Chem.* **276:**19723–19728
11. Grubb, B.R., Paradiso, A.M., Boucher, R.C. 1994. Anomalies in ion transport in CF mouse tracheal epithelium. *Am. J. Physiol.* **267:**C293–C300
12. Hall, R.A., Ostedgaard, L.S., Premont, R.T., Blitzer, J.T., Rahman, N., Welsh, M.J., Lefkowitz, R.J. 1998. A C-terminal motif found in the beta2-adrenergic receptor, $P2Y_1$ receptor and cystic fibrosis transmembrane conductance regulator determines binding to the Na^+/H^+ exchanger regulatory factor family of PDZ proteins. *Proc. Natl. Acad. Sci. USA* **95:**8496–8501
13. Jayaraman, S., Haggie, P., Wachter, R.M., Remington, S.J., Verkman, A.S. 2000. Mechanism and cellular applications of a green fluorescent protein-based halide sensor. *J. Biol. Chem.* **275:**6047–6050
14. Jiang, Q., Li, J., Dubroff, R., Ahn, Y.J., Foskett, J.K., Engelhardt, J., Kleyman, T.R. 2000. Epithelial sodium channels regulate cystic fibrosis transmembrane conductance regulator chloride channels in *Xenopus* oocytes. *J. Biol. Chem.* **275:**13266–13274
15. Kartner, N., Augustinas, T., Jensen, T.J., Naismith, A.L., Riordan, J.R. 1992. Mislocalization of deltaF508 CFTR in cystic fibrosis sweat gland. *Nature Genetics* **1:**321–327
16. Kizer, N.L., Vandorpe, D., Lewis, B., Bunting, B., Russell, J., Stanton, B.A. 1995. Vasopressin and cAMP stimulate electrogenic chloride secretion in an IMCD cell line. *Am. J. Physiol.* **268:**F854–F861
17. Konstas, A.A., Koch, J.P., Tucker, S.J., Korbmacher, C. 2002. Cystic fibrosis transmembrane conductance regulator-dependent up-regulation of Kir1.1 (ROMK) renal K+ channels by the epithelial sodium channel. *J. Biol. Chem.* **277:**25377–25384
18. Korbmacher, C., Segal, A.S., Fejes-Toth, G., Giebisch, G., Boulpaep, E.L. 1993. Whole-cell currents in single and confluent M-1 mouse cortical collecting duct cells. *J. Gen. Physiol.* **102:**761–793
19. König, J., Schreiber, R., Voelcker, T., Mall, M., Kunzelmann, K. 2001. CFTR inhibits ENaC through an increase in the intracellular Cl^- concentration. *EMBO Reports* **2:**1–5
20. Köttgen, M., Busch, A.E., Hug, M.J., Greger, R., Kunzelmann, K. 1996. N-acetyl-L-cysteine and derivatives activate Cl^- conductances in epithelial cells. *Pfluegers Arch.* **431:**549–555
21. Kunzelmann, K. 2003. ENaC is inhibited by an increase in the intracellular Cl^- concentration mediated through activation of Cl^- channels. *Pfluegers Arch.* **445:**505–512
22. Kunzelmann, K., Boucherot, A. 2001. Mechanism of the inhibition of epithelial Na^+ channels by CFTR and purinergic stimulation. *Kidney Int.* **60:**455–461
23. Kunzelmann, K., Mall, M. 2002. Electrolyte transport in the colon: Mechanisms and implications for disease. *Physiol. Rev.* **82:**245–289
24. Kunzelmann, K., Mall, M. 2003. Pharmacotherapy of the ion transport defect in cystic fibrosis: Potential role of P2Y2 receptor agonists. *Am. J. Resp. Med.* **2:**299–329
25. Kunzelmann, K., Mall, M., Briel, M., Hipper, A., Nitschke, R., Ricken, S, Greger, R. 1997. The cystic fibrosis transmembrane conductance regulator attenuates the endogenous Ca^{2+} activated Cl^- conductance in *Xenopus* ooyctes. *Pfluegers Arch.* **434:**178–181
26. Kunzelmann, K., Schreiber, R., Nitschke, R., Mall, M. 2000. Control of epithelial Na^+ conductance by the Cystic Fibrosis Transmembrane Conductance Regulator. *Pfluegers Arch.* **440:**193–201
27. Letz, B., Ackermann, A., Canessa, C.M., Rossier, B.C., Korbmacher, C. 1995. Amiloride-sensitive sodium channels in confluent M-1 mouse cortical collecting duct cells. *J. Membrane Biol.* **148:**127–141
28. Letz, B., Korbmacher, C. 1997. cAMP stimulates CFTR-like Cl^- channels and inhibits amiloride-sensitive Na^+ channels in mouse CCD cells. *Am. J. Physiol.* **272:**C657–C666
29. Mall, M., Bleich, M., Greger Schreiber, R., Kunzelmann, K. 1998. The amiloride inhibitable Na^+ conductance is reduced by CFTR in normal but not in CF airways. *J. Clin. Invest* **102:**15–21
30. Mall, M., Bleich, M., Kühr, J., Brandis, M., Greger, R., Kunzelmann, K. 1999. CFTR-mediated inhibition of amiloride sensitive sodium conductance by CFTR in human colon is defective in cystic fibrosis. *Am. J. Physiol.* **277:**G709–G716
31. Meyer, K., Korbmacher, C. 1996. Cell swelling activates ATP-dependent voltage-gated chloride channels in M-1 mouse cortical collecting duct cells. *J. Gen. Physiol.* **108:**177–193
32. Moyer, B.D., Denton, J., Karlson, K.H., Reynolds, D., Wang, S., Mickle, J.E., Milewski, M., Cutting, G.R., Guggino, W.B., Li, M., Stanton, B.A. 1999. A PDZ-interacting domain in CFTR is an apical membrane polarization signal. *J. Clin. Invest* **104:**1353–1361
33. Moyer, B.D., Duhaime, M., Shaw, C., Denton, J., Reynolds, D., Karlson, K.H., Pfeiffer, J., Wang, S., Mickle, J.E., Milewski, M., Cutting, G.R., Guggino, G.R., Li, M., Stanton,

B.A. 2000. The PDZ interacting domain of CFTR is required for functional expression in the apical plasma membrane. *J. Biol Chem.* **275:**27069–27074

34. Oceandy, D., McMorran, B.J., Smith, S.N., Schreiber, R., Kunzelmann, K., Alten, E.W.F., Hume, D.A., Wainwright, B.J. 2002. Gene complementation of airway epithelium in the cystic fibrosis mouse is necessary and sufficient to correct the pathogen clearance and inflammatory abnormalities. *Hum. Mol. Genet.* **11:**1059–1067
35. Ogura, T., Furukawa, T., Toyozaki, T., Yamada, K., Zheng, Y.J., Katayama, Y., Nakaya, H., Inagaki, N. 2002. CIC-3B, a novel CIC-3 splicing variant that interacts with EBP50 and facilitates expression of CFTR-regulated ORCC. *FASEB J.* **16:**863–865
36. Park, M., Ko, S.B., Choi, J.Y., Muallem, G., Thomas, P.J., Pushkin, A., Lee, M.S., Kim, J.Y., Lee, M.G., Muallem, S., Kurtz, I. 2002. The cystic fibrosis transmembrane conductance regulator interacts with and regulates the activity of the HCO_3^- salvage transporter human Na^+-HCO_3^- cotransport isoform 3. *J. Blol. Chem.* **277:**50503–50509
37. Raghuram, V., Hormuth, H., Foskett, J.K. 2003. A kinase-regulated mechanism controls CFTR channel gating by disrupting bivalent PDZ domain interactions. *Proc. Natl. Acad. Sci. USA* **100:**9620–9625
38. Schreiber, M., Mürle, B., Sun, J., Kunzelmann, K. 2003. Electrolyte transport in the mouse trachea: role of luminal K^+ conductance. *J. Membrane Biol.* **189:**143–151
39. Schreiber, R., König, J., Kunzelmann, K. 2003. Impact of Cl^- but not osmotic swelling on inhibition of Na^+ absorption by purinergic stimulation and activation of CFTR. *J. Membrane Biol.* **192:**101–110
40. Shen, B.Q., Finkbeiner, W.E., Wine, J.J., Mrsny, R.J., Widdicombe, J.H. 1994. Calu-3: a human airway epithelial cell line that shows cAMP-dependent Cl^- secretion. *Am. J. Physiol.* **266:**L493–L501
41. Short, D.B., Trotter, K.W., Reczek, D., Kreda, S.M., Bretscher, A., Boucher, R.C., Stutts, M.J., Milgram, S.L. 1998. An apical PDZ protein anchors the cystic fibrosis transmembrane conductance regulator to the cytoskeletonr. *J. Biol. Chem.* **273:**19797–19801
42. Sun, F., Hug, M.J., Bradbury, N.A., Frizzell, R.A. 2000. Protein kinase A associates with cystic fibrosis transmembrane conductance regulator via an interaction with ezrin. *J. Biol. Chem.* **275:**14360–14366
43. Sun, F., Hug, M.J., Lewarchik, C.M., Yun, C., Bradbury, C.A., Frizzell, R.A. 2000. E3KARP mediates the association of ezrin and PKA with CFTR in airway cells. *J. Biol. Chem.* **275:**29539–29546
44. Swiatecka-Urban, A., Duhaime, M., Coutermarsh, B., Karlson, K.H., Collawn, J., Milewski, M., Cutting, G.R., Guggino, W.B., Langford, G, Stanton, B.A. 2002. PDZ domain interaction controls the endocytic recycling of the cystic fibrosis transmembrane conductance regulator. *J. Biol. Chem.* **277:**40099–40105
45. Taouil, K., Hinnrasky, J., Hologne, C., Corlieu, P., Klossek, J.M., Puchelle, E. 2003. Stimulation of beta 2-adrenergic receptor increases cystic fibrosis transmembrane conductance regulator expression in human airway epithelial cells through a cAMP/protein kinase A-independent pathway. *J. Biol. Chem.* **278:**17320–17327
46. Wang, S., Raab, R.W., Schatz, P.J., Guggino, W.B., Li, M. 1998. Peptide binding consensus of the NHE-RF-PDZ1 domain matches the C-terminal sequence of cystic fibrosis transmembrane conductance regulator (CFTR). *FEBS. Lett.* **427:**103–108
47. Wang, S., Yue, H., Derin, R.B., Guggino, W.B., Li, M. 2000. Accessory protein facilitated CFTR-CFTR interaction, a molecular mechanism to potentiate the chloride channel activity. *Cell* **103:**169–179
48. Wei, L., Vankeerberghen, A., Cuppens, H., Cassiman, J.J., Droogmans, G., Nilius, B. 2001. The C-terminal part of the R-domain, but not the PDZ binding motif, of CFTR is involved in interaction with Ca^{2+}-activated Cl^- channels. *Pfluegers Arch.* **442:**280–285